Boundary Method for Shape Design Sensitivity Analysis in Solving Free-Surface Flow Problems

Joo Ho Choi*
School of Aerospace and Mechanical Engineering, Hankuk Aviation University, 200-1 Hwajon-Dong, Dukyang-Ku, Goyang-City, Gyunggi-Do 412-791, Korea
H. G. Kwak
Department of Aerospace and Mechanical Engineering, Hankuk Aviation University, 200-1 Hwajon-Dong, Dukyang-Ku, Goyang-City, Gyunggi-Do 412-791, Korea
R. V. Grandhi
Department of Mechanical and Materials Engineering, Wright State University, 3640 Colonel Glenn Highway, Dayton, OH, 45435, USA

An efficient boundary-based optimization technique is applied in the numerical computation of free surface flow problems, by reformulating them into the equivalent optimal shape design problems. While the sensitivity in the boundary method has mainly been calculated using the boundary element method (BEM) as an analysis means, the finite element method (FEM) is used in this study because of its popularity and easy-to-use features. The advantage of boundary method is that the design velocity vectors are needed only on the boundary, not over the whole domain. As such, a determination of the complicated domain design velocity field, which is necessary in the domain method, is eliminated, thereby making the process easy to implement and efficient. Seepage and supercavitating flow problem are chosen to illustrate the accuracy and effectiveness of the proposed method.

Key Words: Boundary Method, Shape Design Sensitivity Analysis, Shape Optimization, Free Surface Flow, Seepage, Supercavitation

1. Introduction

Shape optimization problems model geometric data, such as the boundary or interface shape, as the design variables. Because the shape should be altered during the optimization procedure, this is known to be more challenging than conventional sizing design problems. Due to the importance and superiority of shape optimization techniques, there has been a lot of research focused on the theoretical and technical development of the techniques over the past three decades (Haftka and Grandhi, 1986; Kwak, 1994). Now the focus is on the application of these techniques.

In a shape optimization problem, the most popular algorithm involves the use of gradient values to obtain an optimum shape. Though it is well known that the gradient can be easily computed by using finite difference method (FDM), the cost of computation becomes prohibitively expensive for the large number of design parameters. Besides, the FDM often produces erroneous results and leads to a local minimum as will be shown in this paper. Therefore, this research concentrates on an efficient way for gradient computation, which is known as shape design sensitivity analysis (DSA). Material derivative concept and adjoint state equation are two common

* Corresponding Author,
E-mail: jhchoi@hau.ac.kr
TEL: +82-2-300-0117; **FAX**: +82-2-3158-2131
School of Aerospace and Mechanical Engineering, Hankuk Aviation University, 200-1 Hwajon-Dong, Dukyang-Ku, Goyang-City, Gyunggi-Do 412-791, Korea. (Manuscript **Received** June 29, 2005; **Revised** November 12, 2005)

techniques used in the shape DSA.

The theory of shape DSA was pioneered by a number of researchers such as Zolesio (1981), Rousselet and Haug (1981), Choi and Haug (1983), and Dems and Mroz (1984). Numerical implementation was followed and divided in two directions - domain and boundary approach - depending on the form of the sensitivity formula. In the domain approach, the performance function was defined over the shape domain and the sensitivity was also expressed in a domain integral form. The finite element method (FEM) was used as analysis means in the numerical implementation. This approach was mostly employed for the study of optimization of elastic structures (Choi and Seong, 1986; Chang et al., 1995; Hardee et al., 1999), and is now established as a main stream technique in the shape DSA. The domain approach, however, has a drawback in that the shape variation vector, which is also called the design velocity field, should be defined over the whole domain. Recalling that the domain shape is uniquely defined by the boundary only, an arbitrary domain design velocity field should be defined by any means such that it conforms to the boundary shape variation. To this end, a set of auxiliary elasticity problems, called the boundary displacement method, should always be solved under the given boundary shape variation (Yao and Choi, 1989), which increases computing effort and time substantially. If the optimization involves a potential flow problem as in the case of this paper, inefficiency is more severe because two problems of different disciplines should be solved at the every iteration. All of this complexity comes from the sensitivity expressed in a domain integral form. On the other hand, a boundary approach in which sensitivity is expressed in a boundary integral form has been studied as an alternative (Burczyski and Adamczyk, 1985; Choi and Kwak, 1988; Park et al., 1989; Meric, 1995). Since the sensitivity requires only the boundary shape variation, the domain shape variation is not necessary in this method. Therefore, additional analysis like the boundary displacement method is not required either, which is the biggest advantage of the boundary approach. The boundary element method (BEM) has been used for analysis because it does not require meshing of the entire domain and provides an accurate boundary solution. The boundary approach, however, is much less focused than the domain approach because the BEM has limited applications, and is accordingly less popular than the FEM.

In this paper, it is shown that the boundary approach is also implemented excellently while employing the FEM as analysis means. Thanks to the advances in meshing techniques of the FEM, comparable accuracy to the BEM can be achieved by using dense meshing near the boundary. Domain mesh generation, which was one of the drawbacks of the FEM, is no longer an issue due to powerful and convenient auto-meshing abilities. Then, the boundary approach combined with the FEM becomes much more attractive choice. Despite these facts, no study has been done previously in this direction.

Two free surface flow problems - seepage in a dam and supercavitating flow due to a cavitator with extreme high speed underwater - are considered to illustrate the efficiency of the proposed method, even though the method is not limited to this set of problems. It is well known that in the free surface flow problems, the number of free-boundary conditions is one more than the number of boundary conditions required by the governing boundary value problem. The problem, however, can be reformulated into the equivalent shape optimization problem of finding the boundary shape that minimizes a norm of the residual of one of the free-surface conditions, subject to the boundary value problem with the remaining free-surface conditions imposed. While the numerical methods for free-surface potential flow are now pretty mature (for an overview, see Reference (Tsai and Yue, 1996)), and many dedicated techniques have been developed so far, applications of shape optimization technique are found relatively rare. In reference (George, 1997), jet impingement problem was considered and solved by discrete DSA which is to compute sensitivity based on the finite dimensional state equations, hence, does not allow use of existing analysis code. In reference (Karkkainen et al., 1999), the

same problem as (George, 1997) was studied but the continuum DSA was used for the sensitivity analysis. The focus was on the comparison of the shape optimization technique with the trial type methods. In reference (Leontieva and Huacasi, 2001), seepage problem was considered while the BEM and discrete approach was employed. In reference (Van Brummelen1 and Segal, 2003), flow over an obstacle in a channel was studied with an emphasis on the convergence behavior for sub-critical and super-critical flow during the optimization process.

In this paper, commercial software ANSYS is used to solve the potential flow problem. Objective function and its sensitivity are computed by the mathematical package MATLAB using the solutions from ANSYS. The optimization is conducted by using the software VisualDOC in which the cost and gradients are computed by linking with the MATLAB functions. Some implementation issues for the sensitivity analysis and optimization procedure are also addressed in the two example problems.

2. Equivalent Shape Optimization for Free Surface Flow Problems

In this section, the governing equations as well as boundary conditions for the two free surface problems - seepage and supercavitation - are stated, followed by transforming them into the equivalent shape optimization problems. In both the problems, physics of the problem is very simple - the flow is assumed to be potential (irrotational and inviscid) and stationary (steady-state).

The first problem is seepage in a dam, in which water permeates through the cross section of the dam due to the pressure difference. The purpose is to find the shape of wetted part of the dam, which is an important factor in the design of a dam. The problem was considered in (Leontieva and Huacasi, 2001), and is defined in Figure 1, in which u denotes the piezometric potential, and u_s and u_n are the tangential and normal component of the seepage velocity on the boundary, respectively. The permeability coefficient is assumed as unit value for simplicity. As shown in

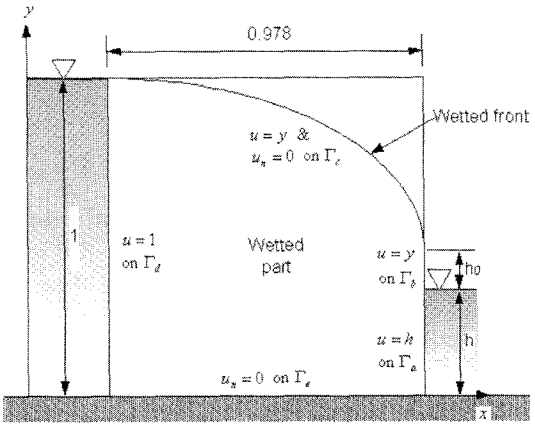

Fig. 1 Seepage problem

the figure, duplicate conditions are imposed at the boundary of wetted front, while the shape of that boundary is not known a priori. The problem can be transformed into the equivalent shape optimization, which is to find the shape of the boundary Γ_c that minimizes square error of one of the boundary conditions. In this paper, the condition that the potential u should be the same as the height y is chosen for this purpose. Then the objective function, which is named as potential difference integral, is

$$\Psi=\int(u-y)^2 ds \tag{1}$$

The potential u should satisfy the following regular boundary conditions.

$$\begin{aligned} &u=h \quad \text{on } \Gamma_a \\ &u=y \quad \text{on } \Gamma_b \\ &u_n=0 \quad \text{on } \Gamma_c \\ &u=1 \quad \text{on } \Gamma_d \\ &u_n=0 \quad \text{on } \Gamma_e \end{aligned} \tag{2}$$

where h is 0.196.

Next problem is a supercavitating flow arising underwater. This occurs when a projectile, like a torpedo, is moving with high speed underwater. At sufficiently high velocity, a huge cavity is created behind the nose of the projectile, covering the body such that it resides within the air pocket, while only the nose of the projectile is wetted. In this respect, the nose of the projectile is called

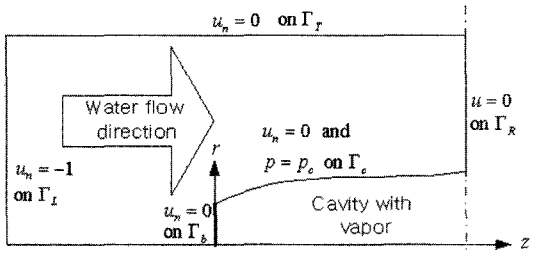

Fig. 2 Supercavitiating flow problem

cavitator. The problem is described in Figure 2, in which the parameters are non-dimensionalized for the sake of simplicity. More details of the supercavitation problem and its assumptions are well described in Ref (Choi et al., 2005). A similar study can also be found by Kirschner (Kirschner et al., 1995) in which the BEM was implemented for analysis. In Figure 2, u denotes the velocity potential, and u_s and u_n are the tangential and normal components of fluid velocity on the boundary, respectively. In this problem, the flow is assumed to be axi-symmetric. Water flows in the axial direction with a unit velocity from the left to the right. A cavitator, which is a disk with unit radius denoted as Γ_b, is located at the origin. The cavity is then formed to the right of the disk as shown in the figure. Assuming symmetry of the cavity shape, only left half of the cavity is considered for simplicity. At the cavity boundary Γ_c, two conditions are imposed simultaneously, which are impermeability and constant pressure, whereas the shape of Γ_c is not known a priori. The constant pressure condition states that the pressure p along the cavity boundary should be equal to the vapor pressure p_c, which leads to the following equation.

$$p-p_c=1+\sigma-u_s^2=0 \tag{3}$$

where σ is the cavitation number defined by

$$\sigma=\frac{p_0-p_c}{\frac{1}{2}\rho U_0^2} \tag{4}$$

In equation (4), p_0, ρ and U_0 are the upstream pressure, the density of the water and the upstream velocity, respectively. The objective func tion for the equivalent shape optimization problem is posed as the pressure difference integral as follows.

$$\Psi=\int_{\Gamma_c}(1+\sigma-u_s^2)^2 r ds \tag{5}$$

which is the integral of square error of the second boundary condition $p=p_c$. Note here that the radius r appears in the integral of the objective function due to its axi-symmetric nature. Associated regular boundary conditions are stated as follows:

$$\begin{aligned} u_n&=0 \quad \text{on } \Gamma_b \\ u_n&=0 \quad \text{on } \Gamma_c \\ u&=0 \quad \text{on } \Gamma_R \\ u_n&=0 \quad \text{on } \Gamma_T \\ u_n&=0 \quad \text{on } \Gamma_L \end{aligned} \tag{6}$$

In the supercavitating flow, the drag force is obtained by integrating the pressure distribution exerted on the disk surface. Evaluating this force is important because it determines the magnitude of the thrust required to maintain any given cavity shape. In practice, the drag coefficient (drag force divided by the disk area) is evaluated as follows:

$$C_d=(1+\sigma)-2\int_{\Gamma_b}u_s^2 n_z r ds \tag{7}$$

where n_z is the axial component of the unit normal on the boundary Γ_b. Though not used in the optimization, the sensitivity of the drag coefficient is also evaluated in this paper.

3. Design Sensitivity Analysis

3.1 Sensitivity analysis theory

The above optimization problem can be stated in a more general manner by defining the objective function in the form

$$\Psi=\int_{\Gamma}\psi(u, u_n, u_s)\, r ds \tag{8}$$

where Ψ is a function of the potential and its derivatives u_s and u_n on the boundary. Radius r is included only in the case of axisymmetricity. The optimum boundary shape Γ is determined to minimize the objective function (8), while the potential u satisfies the Laplace equation

$$\nabla^2 u=0 \text{ in } \Omega \tag{9}$$

and the boundary conditions

$$\begin{aligned} u&=\bar{u} \text{ on } \Gamma_u \\ u_n&=\bar{u}_n \text{ on } \Gamma_n \end{aligned} \tag{10}$$

where the bar denotes the prescribed value, and Γ_u and Γ_n denote Dirichlet boundary and Neumann boundary, respectively. The design sensitivity analysis (DSA) determines the gradient of the objective function (8) due to the shape variation. In a shape design problem, a popular way to describe shape variation is to use the concept of the material derivative (Zolesio, 1981). Based on this concept, variation of a potential u due to the shape change can be expressed as the material derivative.

$$\frac{Du}{Dt}=\frac{\partial u}{\partial t}+V_i\frac{\partial u}{\partial x_i} \text{ or } \dot{u}=u'+\mathbf{V}\cdot\nabla u \tag{11}$$

where the vector $\mathbf{V}(\mathbf{x})$ is the shape variation vector, which is also called design velocity (Choi and Haug, 1983; Choi and Seong, 1986; Chang et al., 1995; Hardee et al., 1999). The material derivative of the general objective functional Ψ given by (8) is then the required sensitivity. Detail process of the sensitivity formula derivation is not addressed here for brevity, but can be found in (Choi, 1987). The final sensitivity formula for the functional Ψ is then given by

$$\Psi'=\int_\Gamma \psi'(u, w; \mathbf{V})\, r ds \tag{12}$$

where

$$\begin{aligned} \psi'(u, w; \mathbf{V})=&(u_s w_n+u_n w_s)\, V_s+(-u_s w_s+u_n w_n)\, V_n \\ &+(u_n w+\psi)\, DV_s^+-\psi_{u_s} u_s DV_s \end{aligned} \tag{13}$$

In this equation, DV_s and DV_s^+ are the functions of design velocity vector $\mathbf{V}$, given by

$$\begin{aligned} DV_s&=V_{k,s}s_k \\ DV_s^+&=DV_s+\frac{V_r}{r} \end{aligned} \tag{14}$$

In the 2-D case, radius r should be removed in (12) and (14). Then DV_s is the same as DV_s^+ in (14). In (12), w is the adjoint potential which has the adjoint boundary conditions,

$$\begin{aligned} w&=-\psi_{u_n} \text{ on } \Gamma_d \\ w_n&=\bar{w}_n \text{ on } \Gamma_n \end{aligned} \tag{15}$$

where $\bar{w}_n$ is the solution of the following weighted residual equation

$$\begin{aligned} &\int_{\Gamma_n}\bar{w}_n w^* r ds \\ &=\int_{\Gamma_n}(\psi_u w^*+\psi_{u_s} w_s^*)\, r ds, \text{ for } \forall w^* \end{aligned} \tag{16}$$

where w^* is an arbitrary function defined on the boundary. If ψ is a sole function of u, and not of u_s, then $\psi_{u_s}=0$, and $\bar{w}_n$ becomes simply ψ_u. The symbols ψ_u, ψ_{u_s} and ψ_{u_n} appearing in (13) and (16) are derivatives with respect to u, u_s and u_n, e.g., $\psi_u=\partial\psi/\partial u$. Equation (12) shows that ψ' is a function of the primal potential u, adjoint potential w and the design velocity vector $\mathbf{V}$. The primal solution for u is obtained from the boundary condition (10). The adjoint solution for w is obtained from the adjoint boundary condition (15), which is to solve the same problem only with different boundary conditions. Thus, in practice, solving the adjoint problem requires only a small increase in computational time because the problem is already set up to solve for the potential u. This approach is called the boundary-based method since the sensitivity formula is always expressed in a boundary integral form, and hence, leads to the evaluation only on the boundary.

The derived sensitivity formula (12) is used for obtaining sensitivity values of the functionals such as potential difference integral (1), pressure difference integral (5) or drag coefficient (7). For the potential difference integral, however, the following expression should be added in the sensitivity formula due to the presence of y, which is the material derivative of $(u-y)^2$ with respect to y

$$\int -2(u-y)\, V_y ds \tag{17}$$

For the drag coefficient, n_z, which is the axial component of the unit normal vector on the boundary, is included. Then the contribution due to the material derivative of this variable should be added in the sensitivity formula, which is

$$2\int u_s^2 DV_n s_z r ds \tag{18}$$

where s_z is axial component of the unit tangent vector on the boundary, and

$$DV_n = V_{k,s} n_k \tag{19}$$

3.2 Overall procedure

Based on the derived sensitivity formula, one can carry out shape DSA, which evaluates gradients of the response with respect to each design parameter. In practice, shape is generally expressed by a number of geometric functions and their associated parameters. Then the design variables are those finite parameters that control the shape. If we denote the design parameter set as $\mathbf{b}=\{b_1, b_2, \cdots, b_n\}$, the boundary shape, i.e., the coordinates of the boundary, is a function of these parameters as follows:

$$\mathbf{x}=\mathbf{x}(\mathbf{b}),\ \mathbf{x}\subset\Gamma \tag{20}$$

The shape variation vector $\mathbf{V}$ appearing in the sensitivity formula is related by the design parameters as

$$\delta\mathbf{x}=\sum_{i=1}^{n}\frac{\partial\mathbf{x}}{\partial b_i}\delta b_i=\sum_{i=1}^{n}\mathbf{V}_i\delta b_i \tag{21}$$

which states that the shape variation vector is the change of the point $\mathbf{x}$ on the boundary due to the variation of each design parameter. Therefore, n sets of the shape variation vector are necessary. After applying this expression into the general formula (12), the sensitivity formula eventually becomes

$$\begin{aligned}\Psi' &= \sum_{i=1}^{n}\int_{\Gamma}\psi'\left(u,\ w,\ \frac{\partial\mathbf{x}}{\partial b_i}\right)ds\cdot\delta b_i \\ &= \sum_{i=1}^{n}\int_{\Gamma}\psi'(u,\ w,\ \mathbf{V}_i)\,ds\cdot\delta b_i \\ &= \sum_{i=1}^{n}GRAD_i\cdot\delta b_i\end{aligned} \tag{22}$$

where $GRAD_i$ is the gradient value for the design parameter b_i, which is used in the optimization routine. Once the boundary shape is given, a potential flow analysis can be performed under the given boundary conditions. In this study, the commercial package ANSYS is used for the implementation of the analysis. Since ANSYS does not have the capability to solve the potential flow problem, the analogy between thermal conduction analysis and potential flow analysis is used in this research. Then the results of thermal analysis are transformed by making use of the similarity between the temperature and the velocity potential in the two types of analyses. An 8-node quadrilateral element PLANE77 is chosen for the analysis. In the calculation of the sensitivity, MATLAB is employed. The overall procedure for the sensitivity calculation is given in Figure 3.

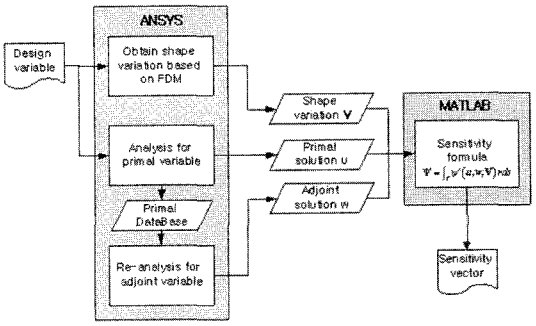

Fig. 3 Overall procedure for sensitivity calculation

3.3 Shape representation and calculation of design velocity vector

Shape is usually expressed by a set of geometric functions such as line, arc, and splines. In this case, the design to be determined is a finite number of design parameters used in the geometric functions. If the design parameter set is denoted as $\mathbf{b}=\{b_1, b_2, \cdots, b_n\}$, the boundary shape, i.e., the coordinates of the boundary, is a function of these parameters. Then, the design velocity vector $\mathbf{V}$ is obtained by differentiating this function with respect to the design parameters. This requires, however, complex manipulation of the functions. An easier way is to employ the finite difference concept only for obtaining the design velocity, which is to generate geometric model for each perturbed design parameter, and calculate the difference of the shape. The concept has been introduced by Hardee et al.(1999). Then the shape variation vector becomes

$$\mathbf{V}_i(\mathrm{x})=\frac{\partial\mathbf{x}}{\partial b_i}\approx\frac{1}{\Delta b_i}\{\mathbf{x}(\mathbf{b}+\Delta b_i\mathbf{e}_i)-\mathbf{x}(\mathbf{b})\} \tag{23}$$

where $\mathbf{e}_i$ denotes the unit vector in the i'th design parameter direction. In fact, this is calculated for each node on the boundary of the FE model.

Since the design velocity vector is necessary only on the boundary, the boundary mesh is sufficient to compute it. The loss of accuracy in this approach is ignorable since we perturb only the geometry, which is distinguished from the original FDM that carries out the entire analysis for each perturbed design. The computing time is also negligible because there is neither domain meshing nor the equation solving process. This approach has definite advantage when compared to the domain-based method. In the domain-based method, an 'auxiliary' elasticity problem should be solved merely for the purpose to determine design velocity vector over the domain under a specified boundary shape variation. This is called the boundary displacement (Yao and Choi, 1989). In the boundary method, however, this is not necessary, which makes the process much simpler and easier.

4. Implementing Design Sensitivity Analysis

The numerical computation of the sensitivity based on the shape DSA method is carried out for the two example problems. The main interest is on the accuracy of the sensitivity values obtained by the method. Since there is no exact solution available for the example problems, the sensitivity values are compared with the values obtained by the finite difference method (FDM), which is to calculate sensitivity by perturbing each design parameter by a small magnitude. Three cases of perturbation ranging from 1%, 0.5% and 0.1% of the design parameter magnitude are tried to check if the FDM sensitivity converges consistently. If so, it is regarded as correct, and used for the comparison with the DSA sensitivity. A ratio is defined, which is the DSA sensitivity divided by the FDM sensitivity multiplied by 100. If the ratio is 100, the two values are identical and the DSA sensitivity is regarded as accurate. The seepage and cavity boundary are represented using the B-spline function in this study.

4.1 DSA implementation for seepage problem

The design parameters are the heights of the seepage boundary at the 5 equally-spaced points including the right end while the height of the left end is fixed. Two different initial shapes - straight line and wavy line - are tried in the sensitivity evaluation. The finite element models are generated automatically by free meshing function of ANSYS as given in Figure 4 for the straight and wavy seepage line. The sensitivity values of the potential difference integral are compared in Table 1. Note that in the case of FDM sensitivity, 6 more analyses are carried out to compute sensitivity, while the DSA sensitivity requires about 0.5 more analysis time is needed for the adjoint

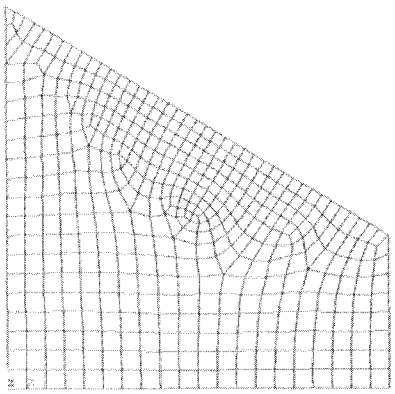

(a) Straight line model

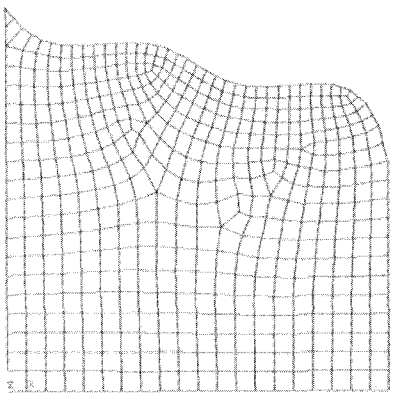

(b) Wavy line model

Fig. 4 Two finite element models in the seepage problem

Table 1 Sensitivity comparison in the seepage problem

(a) Straight line

function	design	FDM (1%)	FDM (0.5%)	FDM (0.1%)	DSA	ratio (%)
Ψ in Eq. (1) =0.00693	0.4	−0.0037	−0.0041	−0.0042	−0.0178	423.65
	0.52	−0.0361	−0.0368	−0.0374	−0.0375	100.24
	0.64	−0.0321	−0.0329	−0.0335	−0.0336	100.45
	0.76	−0.0252	−0.0258	−0.0263	−0.0264	100.39
	0.88	−0.0123	−0.0129	−0.0133	−0.0135	100.99
	1	−0.0094	−0.0095	−0.0095	−0.0100	104.64

(b) Wavy line

function	design	FDM (1%)	FDM (0.5%)	FDM (0.1%)	DSA	ratio (%)
Ψ in Eq. (1) =0.00777	0.6	−0.0117	−0.0115	−0.0123	0.0320	−265.11
	0.8	0.0798	0.0785	0.0774	0.0769	99.67
	0.8	0.0117	0.0107	0.0103	0.0099	100.63
	0.9	0.0206	0.0196	0.0187	0.0179	96.70
	0.9	−0.0226	−0.0238	−0.0243	−0.0245	99.45
	1	0.0219	0.0215	0.0211	0.0257	122.14

solution. The values of the FDM sensitivity for the three perturbation values agree well with each other and that of DSA sensitivity, which shows that the DSA sensitivity is accurate. The overall accuracies are also fine in both the straight and wavy line cases. However, the accuracies of the first design parameter, which is the height at the right end, are found bad in common. The reason might be attributed to the fact that the gradient variables such as u_n, u_x and u_y are not accurate at the corner, which affects the accuracy of the sensitivity.

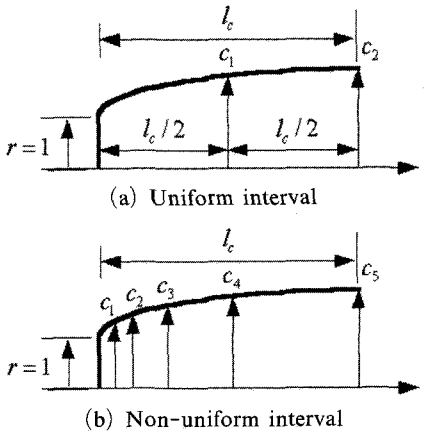

Fig. 5 Design parameters for the cavity shape

4.2 DSA implementation for supercavitation problem

Sensitivity values are computed for two functions, pressure difference integral and drag coefficient, in the supercavitating flow problem. To describe the cavity shape, two height parameters c_1 and c_2, which are located at the middle and the end of the cavity, are considered (see Figure 5(a)). The length of the cavity l_c and the cavitation number σ, which is a non-shape parameter, are considered as well. The design parameters are, therefore, c_1, c_2, l_c and σ. The cavity length is 5 and the slope at the end of the cavity is assigned a direction vector (1, 0) in order to

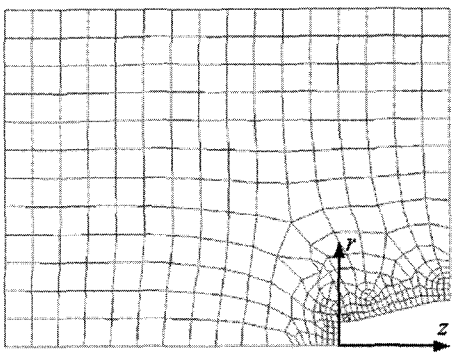

Fig. 6 Initial finite element model with free-meshing

Table 2 Sensitivity comparison of the two functions with the free-mesh model in the supercavitation problem

function	design parameter	design value	FDM (1%)	FDM (0.5%)	FDM (0.1%)	DSA	ratio (%)
Ψ in Eq. (5) =0.2804	c_1	1.50	−0.362	−0.176	0.324	−0.681	−210.0
	c_2	2.00	0.629	0.665	−3.353	0.534	−15.9
	l_c	5.00	−0.074	−0.080	−0.394	−0.010	2.6
	σ	0.16	−0.209	−0.211	−0.212	−0.212	100.1
C_d in Eq. (7) =0.5976	c_1	1.50	−0.371	−1.398	−1.029	0.529	−51.4
	c_2	2.00	1.564	−0.963	−9.183	−0.126	1.4
	l_c	5.00	−0.251	−0.884	−3.555	−0.030	0.8
	σ	0.16	1.000	1.000	1.000	1.000	100.0

Table 3 Sensitivity comparison of the two functions with the mapped-mesh model in the supercavitation problem

function	design parameter	design value	FDM (1%)	FDM (0.5%)	FDM (0.1%)	DSA	ratio (%)
Ψ in Eq. (5) =0.2715	c_1	1.50	−0.642	−0.642	−0.642	−0.672	104.6
	c_2	2.00	0.536	0.533	0.532	0.544	102.2
	l_c	5.00	−0.063	−0.063	−0.064	−0.020	31.7
	σ	0.16	−0.209	−0.211	−0.212	−0.212	100.1
C_d in Eq. (7) =0.5671	c_1	1.50	0.616	0.617	0.618	0.564	91.3
	c_2	2.00	−1.156	−0.156	−0.156	−0.137	87.9
	l_c	5.00	−0.034	−0.034	−0.035	−0.043	122.7
	σ	0.16	1.000	1.000	1.000	1.000	100.0

ensure symmetry. Finite element model by free meshing function is shown in Figure 6. To check whether consistent sensitivity is obtained, three perturbation values, 1%, 0.5% and 0.1%, are tried for the FDM. The resulting sensitivity values are compared in Table 2, in which the FDM sensitivity values of the three different perturbations do not agree at all. The reason is that unlike the seepage problem, the auto-meshing produces a quite different mesh for a slight change in shape in this problem. To avoid this, mapped-meshing, which is a more stable mesh pattern, is tried as shown in Figure 7. The sensitivity values are compared in Table 3. The three FDM sensitivity values are now in good agreement, and also agree with the DSA sensitivity. However, the ratio for the design parameter l_c is still inaccurate. This is due to the inaccuracy of the FEM solution for the normal velocities, u_n and w_n, near the cavity corner on the right end boundary Γ_R, which is the symmetry plane. On this boundary, the velocity tends to show a singular behavior

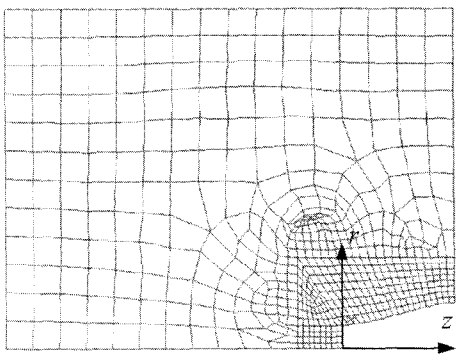

Fig. 7 Initial finite element model with mapped-meshing

unless the cavity shape ends orthogonal to Γ_R. Unlike the other design parameters, l_c yields a non-zero shape variation vector on Γ_R, and hence, produces an inaccurate result. To reduce this behavior, a cavity of a smoother shape having a near-orthogonal corner is considered in which c_1 is 1.8 as shown in Figure 8. The sensitivity comparison of the smoother cavity shape shows

much better accuracy as indicated in Table 4. It is interesting to note that the DSA sensitivitys using the free-mesh model and the mapped-mesh model agree well. This is shown in Table 5. Though mapped-meshing is superior in mesh quality to the free-meshing, it is not advisable because much more human effort is needed for the mesh construction. Free-mesh, however, can be generated easily by employing automatic meshing capability. Since the sensitivity values are the same for the two mesh models, free-mesh can also be employed in the optimization.

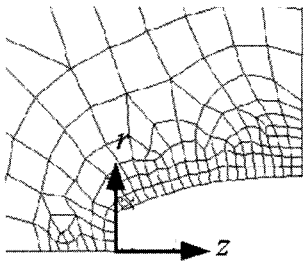

Fig. 8 Mesh model with smoother cavity shape

Table 4 Sensitivity comparison of the two functions with smoother cavity shape in the super-cavitation problem

function	design parameter	FDM (0.1%)	DSA	ratio (%)
Ψ in Eq. (5) =0.1228	c_1	−0.104	−0.119	114.6
	c_2	0.207	0.210	101.6
	l_c	−0.047	−0.055	117.4
	σ	−0.678	−0.679	100.1
C_d in Eq. (7) =0.7373	c_1	0.495	0.475	96.0
	c_2	−0.132	−0.127	96.2
	l_c	−0.044	−0.055	125.3
	σ	1.000	1.000	100.0

Table 5 Sensitivity comparison of the two functions for different mesh model in the supercavitation problem

function	design parameter	DSA free-mesh	DSA map-mesh	ratio (%)
Ψ in Eq. (5)	c_1	−0.681	−0.672	98.7
	c_2	0.534	0.544	102.0
	l_c	−0.010	−0.020	201.0
	σ	−0.212	−0.212	100.0
C_d in Eq. (7)	c_1	0.529	0.564	106.6
	c_2	−0.126	−0.137	109.0
	l_c	−0.030	−0.043	143.5
	σ	1.000	1.000	100.0

5. Implementing Optimization

In this section, implementation of the optimization task using the gradient-based algorithm is discussed. The commercial package VisualDOC is chosen for this purpose. In the gradient computation, the FDM is also used for comparing the result with that of the proposed shape DSA method. In the seepage problem, the optimization is conducted using the design parameters considered in the DSA implementation. The same shape is obtained after optimization from the two initial designs, as shown in Figure 9. The optimization is also conducted using the FDM based sensitivity. Again, the same optimum shape is obtained, but at the expense of 5 times longer computing time in this case. The optimum shape is also compared in Table 6 with the analytical solution given from reference (Leontieva and Huacasi, 2001) which is

$$x=l-\int_0^{\chi}\frac{\mathrm{K}(\sin^2\chi)\sin\chi d\chi}{\sqrt{(1-\alpha\sin^2\chi)(1-\beta\sin^2\chi)}} \qquad 0\le\chi\le\pi/2 \tag{24}$$

$$y=h_0+h+\int_0^{\chi}\frac{\mathrm{K}(\cos^2\chi)\sin\chi d\chi}{\sqrt{(1-\alpha\sin^2\chi)(1-\beta\sin^2\chi)}} \qquad 0\le\chi\le\pi/2 \tag{25}$$

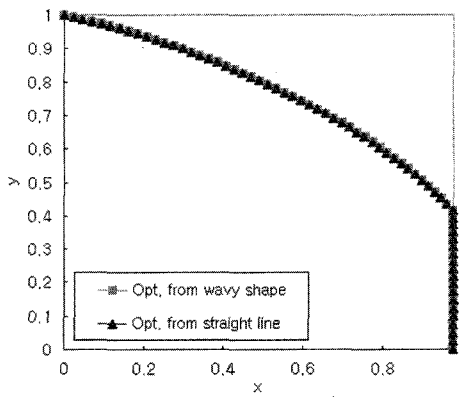

Fig. 9 Optimum shapes in the seepage problem

where $l=0.978$ and $K(\chi)$ denotes the complete elliptic integral of the first kind ; α, $\beta \in (0, 1)$ are parameters that define the problem. In this table, the first column indicates x coordinate of the equally-spaced design parameter points and second column is y coordinate obtained by analytical solution. The third column presents the solution by the DSA. The fourth column includes the ratio of the DSA solution divided by the analytical solution.

In the supercavitation problem, the same design parameters and cavitator used in the DSA study are also used for the optimization. The problem is to find the cavity shape as well as the cavitation number under the given cavity length which is 5 in this case. During the optimization, the free-mesh model is used. The optimum cavity shapes are compared in Figure 10. The upper solid curves are the optimum shapes of the cavity by the DSA method starting from the initial shape of dashed straight line, which is plausible and close to an elliptical shape as can be expected. Unlike the seepage case, wrong optimum shape is obtained by the FDM method in this problem due to the inaccurate sensitivity as can be seen from the grey curve of the figure. In Figure 11, the objective function histories with respect to the number of iterations are plotted for the different approaches. In this figure, "map" and "free" denote mapped-mesh and free-mesh model, respectively. The DSA method for the two mesh models shows almost the same behavior. The DSA methods for the two mesh models as well as the FDM with mapped-mesh model show almost the same behavior. The result for the FDM with free-mesh model, however, does not show convergence, which demonstrates that if the FDM should be used in the optimization for any reason, the free-mesh should be avoided. Instead, the mapped-mesh, though it requires more human effort in construction, should be employed. A number of optimum solutions are investigated for various cavity lengths. The relation between the cavitation number σ and the drag coefficient c_d is then obtained using these results. This is to verify the results of the proposed method with the theoretical result by Logvinovich (1972), which is given by

$$c_d=0.82(1+\sigma) \tag{26}$$

The results are obtained for two numbers of design parameter points, which are $n_c=2$ and 5. Graph of the drag coefficient versus the cavitation number is shown in Figure 12. In this figure,

Table 6 Comparison with the analytical and optimum solution in the seepage problem

x	y		ratio (%)
	Analytical solution	DSA optimum	
0.9780	0.4050	0.4121	101.75
0.8802	0.5282	0.5240	99.20
0.7824	0.6167	0.6140	99.56
0.6846	0.6889	0.6869	99.71
0.5868	0.7505	0.7481	99.68
0.4890	0.8075	0.8040	99.57
0.3912	0.8595	0.8555	99.53
0.2934	0.9030	0.9001	99.68
0.1956	0.9393	0.9403	100.11
0.0978	0.9747	0.9733	99.86

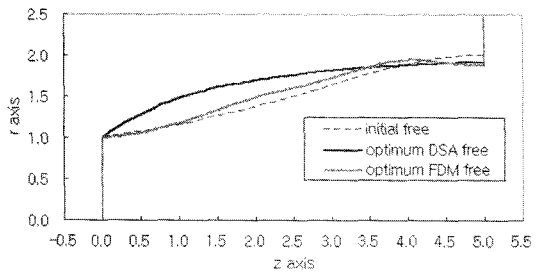

Fig. 10 Initial and optimum cavity shapes in the supercavitation problem

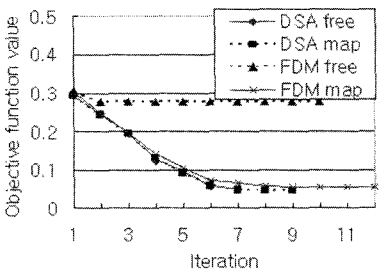

Fig. 11 Objective function history in the supercavitation problem

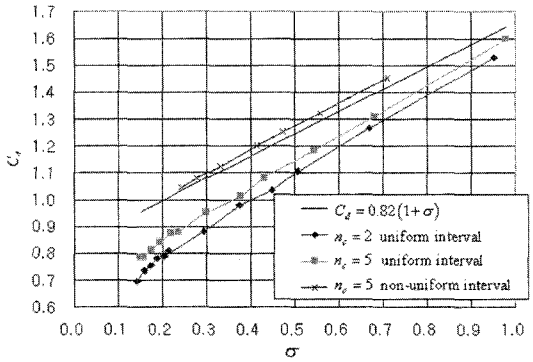

Fig. 12 Comparison between theoretical and numerical results of σ and C_d

the results by the n_c=5 are closer to the analytical solution than the results by the n_c=2. This demonstrates that for a closer result, the number of height parameters should be further increased to accommodate the rapidly varying cavity shape near the beginning of the cavity to reduce the error in prediction. To reflect this more efficiently, a non-uniform interval is examined, which places more parameters at the beginning of the cavity shape as shown in Figure 5(b). The result from this simulation is included in Figure 12 in which the line is found to be much closer to the theoretical line.

6. Discussions and Conclusions

In this study, an efficient boundary-based DSA technique in which the FEM is used for the analysis has been proposed for the optimization process in the potential flow problems. Though the numerical examples considered in this paper are free surface flow problems, this technique can be applied to any kind of shape optimization problem associated with potential flow. Due to the feature that the sensitivity formula is in boundary integral form, the design velocity vectors are needed only on the boundary, and not over the whole domain. Then the surface or boundary mesh generation is sufficient in evaluating the design velocity vector. Unlike the domain method, there is no need to solve an auxiliary elasticity problem in which the domain design velocity fields are determined based on the given boundary shape variation.

A seepage and supercavitation problems are chosen to illustrate the proposed methodology in which the optimum shapes are sought to minimize the square error integral of the one of the duplicate boundary conditions defined on the free boundary. In the study for sensitivity evaluation, the accuracies of the DSA method are compared to those by the FDM. For the both problems, the free-mesh model is employed for the flow analysis, which is conveniently generated using the automatic meshing capability. The results of supercavitation problem, however, indicate that the sensitivity by the FDM is not accurate in the free-mesh model due to the quite different mesh generation for a slight change of the shape in this problem. This is avoided by using mapped-mesh model, which requires more human labor, and hence, is not advisable in practical optimization. Since the sensitivity values by the DSA method are found to agree well whether free-mesh or mapped-mesh is employed, convenient free-mesh is employed during the optimization. The shape optimization result of seepage problem is compared to the analytical solution, and found to have close agreement. Shape optimization is also carried out for supercavitation problem. In this case, optimization by the FDM is carried out for comparison, from which wrong optimum solution is observed. A number of optimizations are investigated for various cavity lengths for validation purposes. The relationship between the cavitation number and drag coefficient is then obtained and compared to the theoretical result. It is found that the results get closer to the analytical solution as the number of design parameters is increased.

References

Burczyski, T. and Adamczyk, T., 1985, "The Boundary Element Formulation for Multiparameter Structural Shape Optimization," *Applied Mathematical Modeling*, Vol. 9, pp. 95~200.

Chang, K. H., Choi, K. K., Tsai, C. S., Chen, C. J., Choi, B. S. and Yu, X., 1995, "Design Sensitivity Analysis and Optimization Tool (DSO)

for Shape Design applications," *Computing Systems in Engineering*, Vol. 6, pp. 151~175.

Choi, J. H. and Kwak, B. M., 1988, "Boundary Integral Equation Method for Shape Optimization of Elastic Structures," *International Journal for Numerical Methods in Engineering*, Vol. 26, pp. 1579~1595.

Choi, J. H., 1987, *Shape Optimal Design Using Boundary Integral Equations*, Ph.D., Thesis, Korea Advanced Institute of Science and Technology, Seoul, Korea.

Choi, J. H., Penmetsa, R. C. and Grandhi, R. V., 2005, "Shape Optimization of the Cavitator for a Supercavitating Torpedo," *Structural and Multidisciplinary Optimization*, Vol. 29, pp. 159~167.

Choi, K. K. and Haug, E. J., 1983, "Shape Design Sensitivity Analysis of Elastic Structures," *Journal of Structural Mechanics*, Vol. 11, pp. 231~269.

Choi, K. K. and Seong, H. G., 1986, "Domain Method for Shape Design Sensitivity Analysis of Built-up Structures," *Computer Methods in Applied Mechanics and Engineering*, Vol. 57, pp. 1~15.

Dems, K. and Mroz, Z., 1984, "Variational Approach by Means of Adjoint Systems to Structural Optimization and Sensitivity Analysis - II : Structure Shape Variation," *International Journal of Solids and Structures*, Vol. 20, pp. 527~552.

George, Mejak., 1997, "Finite Element Solution of a Model Free Surface Problem by the Optimal Shape Design Approach," *International Journal for Numerical Methods in Engineering*, Vol. 40, pp. 1525~1550.

Haftka, R. T. and Grandhi, R. V., 1986, "Structural Shape Optimization - A Survey," *Computer Methods in Applied Mechanics and Engineering*, Vol. 57, pp. 91~106.

Hardee, E., Chang, K. H., Tu, J., Choi, K. K. Grindeanu, I. and Yu, X., 1999, "A CAD-Based Design Parameterization for Shape Optimization of Elastic Solids," *Advances in Engineering Software*, Vol. 30, pp 185~199.

Karkkainen, Kari T. and Tiihonen, Timo., 1999, "Free Surfaces : Shape Sensitivity analysis and Numerical Methods," *International Journal for Numerical Methods in Engineering*, Vol. 44, pp. 1079~1098.

Kirschner, I. N., Kring, D. C., Stokes, A. W., Fine, N. E. and Uhlman, Jr. J. S., 1995, "Supercavitating Projectiles in Axisymmetric Subsonic Liquid flows," *American Society of Mechanical Engineers, Fluids Engineering Division (Publication) FED*, Vol. 210, pp.75~93.

Kwak, B. M., 1994, "A Review on Shape Optimal Design and Sensitivity Analysis," *Journal of Structural Mechanics and Earthquake Engineering, JSCE.*, Vol. 10, pp. 1595~1745.

Leontieva, A. and Huacasi, W., 2001, "Mathematical Programming Approach for Unconfined Seepage Flow Problem," *Engineering Analysis with Boundary Elements*, Vol. 25, pp. 49~56.

Logvinovich, G. V., 1972, *Hydrodynamics of Free-Boundary Flows*. Translated From Russian, Israel Program for Scientific Translations : Jerusalem.

Meric, R. A., 1995, "Differential and Integral Sensitivity Formulations and Shape Optimization by BEM," *Engineering Analysis with Boundary Elements*, Vol. 15, pp. 181~188.

Park, C. W., Yoo, Y. M. and Kwon, K. H., 1989, "Shape Design Sensitivity Analysis of an Axisymmetric Turbine Disk Using the Boundary Element Method," *Computers & Structures*, Vol. 33, pp. 7~16.

Rousselet, B. and Haug, E. J., 1981, Design Sensitivity Analysis of Shape Variation, in E.J. Haug and J. Cea, (eds.), Optimization of Distributed Parameter Structures, Sijthoff-Noordhoff and Alphen aan den Rijn, The Netherlands, pp. 1397~1442.

Tsai, W. and Yue, D. K. P., 1996, "Computation of Nonlinear Free-Surface Flows," *Annual Reviews on Fluid Mechanics*, Vol. 28, pp. 249~278.

Van Brummelen1, E. H. and Segal, A., 2003, "Numerical Solution of Steady Free-Surface Flows by the Adjoint Optimal Shape Design Method," *International Journal for Numerical Methods in Fluids*, Vol. 41, pp. 3~27.

Yao, T. M. and Choi, K. K., 1989, "3-D Shape Optimal Design and Automatic Finite Element

Regridding," *International Journal for Numerical Methods in Engineering*, Vol. 28, pp. 369~384.

Zolesio, J. P., 1981, The Material Derivative (or Speed) Method for Shape Optimization, in E.J. Haug and J. Cea (eds.), Optimization of Distributed Parameters Structures, Sijthoff-Noordhoff and Alphen aan den Rijn, The Netherlands pp. 1152~1194.